

AperTO - Archivio Istituzionale Open Access dell'Università di Torino

Non-newly generated, "immature" neurons in the sheep brain are not restricted to cerebral cortex

This is a pre print version of the following article:

Original Citation:

Availability:

This version is available <http://hdl.handle.net/2318/1653592> since 2018-02-09T11:02:48Z

Published version:

DOI:10.1523/JNEUROSCI.1781-17.2017

Terms of use:

Open Access

Anyone can freely access the full text of works made available as "Open Access". Works made available under a Creative Commons license can be used according to the terms and conditions of said license. Use of all other works requires consent of the right holder (author or publisher) if not exempted from copyright protection by the applicable law.

(Article begins on next page)

This is the author's pre-print of the contribution published as:

Matteo Piumatti, Ottavia Palazzo, Chiara La Rosa, Paola Crociara, Roberta Parolisi, Federico Luzzati, Frederic Lévy, Luca Bonfanti

Paper: Non-newly generated, "immature" neurons in the sheep brain are not restricted to cerebral cortex

JOURNAL OF NEUROSCIENCE, None, 2017, pp: 1781-1817

DOI: 10.1523/JNEUROSCI.1781-17.2017

The publisher's version is available at:

<https://doi.org/10.1523/JNEUROSCI.1781-17.2017>

When citing, please refer to the published version.

Link to this full text:

<http://hdl.handle.net/2318/1653592>

This full text was downloaded from iris-AperTO: <https://iris.unito.it/>

Research Articles: Development/Plasticity/Repair

Non-newly generated, “immature” neurons in the sheep brain are not restricted to cerebral cortex

Matteo Piumatti¹, Ottavia Palazzo¹, Chiara La Rosa^{1,2}, Paola Crociara¹, Roberta Parolisi¹, Federico Luzzati^{1,3}, Frederic Lévy⁴ and Luca Bonfanti^{1,2}

¹Neuroscience Institute Cavalieri Ottolenghi (NICO), Orbassano, Italy

²Department of Veterinary Sciences, University of Turin, Torino, Italy

³Department of Life Sciences and Systems Biology, University of Turin, Italy

⁴UMR INRA, CNRS/Université F. Rabelais, IFCE Physiologie de la Reproduction et des Comportements, Nouzilly, France

Author contributions: M.P., O.P., C.L.R., and P.C. performed research; M.P., O.P., C.L.R., R.P., F. Luzzati, F. Levy, and L.B. analyzed data; F. Luzzati and L.B. designed research; F. Levy and L.B. contributed unpublished reagents/analytic tools; L.B. wrote the paper.

Conflict of Interest: The authors declare no competing financial interests.

the present work has been supported by MIUR-PRIN2015 (grant 2015Y5W9YP), the University of Turin (PhD program in Veterinary Sciences), Fondazione CRT (Bando Ricerca e Istruzione 2014), and the French Agence Nationale pour la Recherche, PLASTMATBEHAV ANR12-BSV7-0017. The Authors thank the Istituto Zooprofilattico del Piemonte, Liguria e Valle D'Aosta and Dr. Alessandra Pecora for technical help in the first phases of the study.

Correspondence to: Luca Bonfanti, DVM, PhD, Department of Veterinary Sciences, Largo Braccini 2, 10095 Grugliasco (TO), University of Turin, Italy, Email: luca.bonfanti@unito.it

1
2
3
4
5
6
7
8
9
10
11
12
13
14
15
16
17
18
19
20
21
22
23
24
25
26
27
28
29
30
31

32
33
34
35
36
37

**Non-newly generated, "immature" neurons
in the sheep brain are not restricted to cerebral cortex**

Abbreviated title: **Immature neurons in the sheep brain**

Matteo Piumatti^{1§}, Ottavia Palazzo^{1§}, Chiara La Rosa^{1,2}, Paola Crociara¹, Roberta Parolisi¹, Federico Luzzati^{1,3}, Frederic Lévy⁴, Luca Bonfanti^{1,2*}

¹ Neuroscience Institute Cavalieri Ottolenghi (NICO), Orbassano, Italy; ² Department of Veterinary Sciences, University of Turin, Torino, Italy; ³Department of Life Sciences and Systems Biology, University of Turin, Italy; ⁴UMR INRA, CNRS/Université F. Rabelais, IFCE Physiologie de la Reproduction et des Comportements, Nouzilly, France

[§] These Authors contributed equally
M.P. present address: Université Libre de Bruxelles (ULB), Institute for Interdisciplinary Research (IRIBHM), Belgium; P.C. present address: Istituto Zooprofilattico Sperimentale del Piemonte Liguria e Valle d'Aosta, Torino, Italy.

* Correspondence to: Luca Bonfanti, DVM, PhD
Department of Veterinary Sciences
Largo Braccini 2
10095 Grugliasco (TO)
University of Turin, Italy
Email: luca.bonfanti@unito.it

Number of Figures: **10**; Number of Tables: **3**
Number of words: Abstract **218**; Introduction **569**; Discussion **1498**

Acknowledgements: the present work has been supported by MIUR-PRIN2015 (grant 2015Y5W9YP), the University of Turin (PhD program in Veterinary Sciences), Fondazione CRT (Bando Ricerca e Istruzione 2014), and the French Agence Nationale pour la Recherche, PLASTMATBEHAV ANR12-BSV7-0017. The Authors thank the Istituto Zooprofilattico del Piemonte, Liguria e Valle D'Aosta and Dr. Alessandra Pecora for technical help in the first phases of the study.

38 **Abstract**

39

40 A newly proposed form of brain structural plasticity consists of non-newly generated, "immature"
41 neurons of the adult cerebral cortex. Similar to newly generated neurons, these cells express the
42 cytoskeletal protein Doublecortin (DCX), yet they are generated prenatally, then remaining in a
43 state of immaturity for long periods. In rodents, the immature neurons are restricted to the
44 paleocortex, whereas in other mammals are found also in neocortex. Here, we analyzed the DCX-
45 expressing cells in the whole sheep brain of both sexes, to search for an indicator of structural
46 plasticity at a cellular level in a relatively large-brained, long-living mammal. Brains from adult and
47 newborn sheep (injected with BrdU and analyzed at different survival times) were processed for
48 DCX, cell proliferation markers (Ki-67, BrdU), pallial/subpallial developmental origin (*Tbr1*, *Sp8*),
49 and neuronal/glial antigens for phenotype characterization. We found immature-like neurons in the
50 whole sheep cortex and in large populations of DCX-expressing cells within the external capsule
51 and the surrounding grey matter (claustrum and amygdala). BrdU and Ki-67 detection at neonatal
52 and adult ages showed that all these DCX+ cells were generated during embryogenesis, not after
53 birth. These results show that the adult sheep, unlike rodents, is largely endowed with non-newly
54 generated neurons retaining immature features, suggesting that such kind of plasticity might be
55 particularly important in large brained, long living mammals.

56 **Significance statement**

57 Brain plasticity is important in adaptation and brain repair. Structural changes span from synaptic
58 plasticity to adult neurogenesis, the latter being highly reduced in large-brained, long-living
59 mammals (e.g., humans). The cerebral cortex contains "immature" neurons, which are generated
60 prenatally then remaining in an undifferentiated state for long periods, being detectable with
61 markers of immaturity. We studied the distribution and developmental origin of these cells in the
62 whole brain of sheep, namely, relatively large-brained, long-living mammals. In addition to the
63 expected cortical location, we also found populations of non-newly generated neurons in several
64 subcortical regions (external capsule, claustrum, amygdala). These results suggests that non-
65 neurogenic, parenchymal structural plasticity might be more important in large mammals with
66 respect to adult neurogenesis.

67 **Introduction**

68 The mammalian central nervous system (CNS) is build up mostly of non-renewable (perennial)
69 neurons whose cell processes are connected physically and functionally in a largely invariant way.
70 Though anatomical invariability is a necessary requisite to assure stability of connections in the
71 neural circuits (Frotscher, 1992), exceptions do exist in the form of cellular modifications referred
72 to as "structural plasticity", affecting the brain anatomy at different levels and degrees (Bonfanti,
73 2006; Theodosios et al., 2008). These exceptions span from formation/elimination of synapses in pre-
74 existing neurons (synaptic plasticity; Bonfanti and Theodosios, 2009; Bailey et al., 2015) to
75 addition/replacement of new neurons (adult neurogenesis; Bonfanti and Peretto, 2011; Aimone et
76 al., 2014). The occurrence, amount, type and location of neural structural plasticity, as well as its
77 reparative capacity, greatly vary in the animal world (Bonfanti, 2011; Grandel and Brand, 2013)
78 and, to a lesser extent, among mammals (Feliciano et al., 2015; Lipp and Bonfanti, 2016). The
79 cytoskeletal protein doublecortin (DCX) is an excellent marker for cells that retain high potential
80 for structural plasticity in the CNS (Gleeson et al., 1999; Nacher et al., 2001). Due to its heavy
81 expression in newly generated neuroblasts and during the early phases of their
82 migration/differentiation, DCX is commonly used as a marker for adult neurogenesis (Brown et al.,
83 2003). Nevertheless, it is now clear that at least a type of neurons located in the layer II of the adult
84 mammalian cerebral cortex, which are not newly generated ("immature neurons", Gomez-Climent
85 et al., 2008), express DCX during adulthood (for review, see Bonfanti and Nacher, 2012; Nacher
86 and Bonfanti, 2015). Current data indicate that the occurrence and distribution of DCX+ cells can
87 substantially vary in brain regions of different mammals (Feliciano et al., 2015; Lipp and Bonfanti,
88 2016), thus suggesting species-specific heterogeneity in the capability to undergo structural
89 plasticity, both neurogenic and non-neurogenic. For instance, the rate of adult neurogenesis
90 decreases in mammals with extended life expectancy (e.g., humans, dolphins and sheep; Sanai et al.,
91 2011; Brus et al., 2013a; Parolisi et al., 2015,2017) if compared with the relatively short-living

laboratory rodents (reviewed in Paredes et al., 2015; Lipp and Bonfanti, 2016). By contrast, the occurrence of cortical layer II immature neurons is higher in rabbits, guinea pigs and cats with respect to rats and mice, extending into neocortical regions in the former and being restricted to paleocortex in the latter (Luzzati et al., 2009; Cai et al., 2009; Xiong et al., 2008). Here, the occurrence of DCX⁺ cells was investigated in sheep (*Ovis aries*) with the idea of analysing the distribution of this indicator of structural plasticity in a relatively long-living mammal endowed with a large-sized, gyrencephalic brain. Sheep possess a brain as large as a macaque monkey and have a similar life span (10/30 years in wild/captivity); also, experimental procedures such as BrdU injection for subsequent immunocytochemical detection of newly generated cells in the brain tissue can be performed in these animals. Neonatal and adult animals treated with BrdU (injected in pregnant ewes in the case of neonates) were studied in order to assess the time of genesis (prenatal vs. postnatal) of the DCX⁺ cells. We show that in the adult sheep brain, in addition to cortical immature neurons, different populations of non-newly generated DCX⁺ cells are consistently present in the external capsule and adjacent regions. Interestingly enough, quantification of these latter cells in neonatal, prepuberal and adult animals showed they are not depleted through ages.

107

108

109

110 **Materials and Methods**

111

112 **Animals, BrdU injections, tissue preparation**

Neonatal, prepuberal and adult animals (Ile de France) were raised at the INRA research center (Nouzilly; Indre et Loire, France). Experiments were conducted on 9 adult (females, 2 year old), 3 prepuberal (males, 4 month old), and 7 neonatal animals (4 males, 3 females, 1 week old; see Table

116 1). Adult ewes were housed in an individual pen (2x1 m) and received four intravenous injections
117 of bromodeoxyuridine (BrdU) during pregnancy (1 injection/day, 20 mg/Kg in 0.9% saline; Sigma-
118 Aldrich, France), a thymidine analogue incorporated into the DNA during the S-phase of the mitotic
119 division. Two days after lambing, ewes were anesthetized with thiopental and decapitated by a
120 licensed butcher in an official slaughterhouse (ethical permissions reported in Brus et al., 2013b).
121 Three different survival times were analyzed in these adult animals: 1, 2 and 4 months (see Brus et
122 al., 2013b). Since all the ewes were pregnant, the intravenous injections of BrdU could allow the
123 molecule to pass to the fetuses and thus being incorporated in their brain. All the lambs used in this
124 study were collected from mothers being injected 3 months before parturition (i.e. at 2-month
125 gestational days). Brains were perfused through both carotid arteries with 2L of 1% sodium nitrite
126 in phosphate buffer saline, followed by 4 L of ice-cold 4% paraformaldehyde solution in 0,1M
127 phosphate buffer at pH 7,4. The brains were then dissected out, cut into blocks and post-fixed in the
128 same fixative for 48h. The tissues were then stored in 30% sucrose. Each hemisphere has been cut
129 into 4 coronal slices (about 1,5 cm thick), embedded in OCT (optimum cutting temperature, Bio-
130 Optica), frozen in isopentane, and stored at -80°C. Cryostat coronal sections (40 µm tick) were cut
131 to be employed in free-floating immunohistochemistry and immunofluorescence procedures. We
132 then obtained the outlines of four levels of interest, representing the whole sheep brain (L1-L4), by
133 combining the analysis of our cryostat sections and photographs from the atlas of Brain
134 Biodiversity Bank of Michigan State University (Fig. 1).

135

136

137 **3.2 Immunohistochemistry**

138 Immunohistochemical reactions were performed on free-floating sections, when necessary, antigen
139 retrieval was performed using citric acid at 90°C for 5-10 minutes. The section were incubated in
140 blocking buffer (2% normal serum, 0,5-1% Triton X-100 in 0,01M PBS, ph 7.4) for 2h at room

141 temperature, then incubated for 24-48 h at 4 °C in a solution of 0.01 M PBS, pH 7.4, containing 0,5-
 142 1% Triton X-100, 2% normal serum and the primary antibodies (see Table 2). Sections were then
 143 incubated with appropriate solutions of secondary antibody: Alexa-488 conjugated goat anti mouse
 144 (1:400, Molecular Probes, Eugene, OR), Alexa-488 conjugated goat anti rabbit (1:400, Molecular
 145 Probes, Eugene, OR), Alexa-488 conjugated donkey anti rat (1:400 Jackson ImmunoResearch,
 146 West Grove, PA), Alexa-555 conjugated goat anti mouse (1:800, Molecular Probes, Eugene, OR),
 147 Alexa-555 conjugated goat anti rabbit (1:800, Molecular Probes, Eugene, OR), Alexa-555
 148 conjugated goat anti guinea pig (1:800, Molecular Probes, Eugene; OR), cyanine 3 (cy3) conjugated
 149 goat anti mouse (1:800, Jackson ImmunoResearch, West Grove, PA), cyanine 3 (cy3) conjugated
 150 goat anti rabbit (1:800, Jackson ImmunoResearch, West Grove, PA), cyanine 3 (cy3) conjugated
 151 donkey anti goat (1:800, Jackson ImmunoResearch, West Grove, PA), Alexa-647 conjugated donkey
 152 anti mouse (1:800, Jackson ImmunoResearch, West Grove, PA), Alexa-647 conjugated donkey anti
 153 rabbit, for 3h at RT. Sections were counterstained with 4',6-diamidino-2-phenylindole (DAPI, KPL,
 154 Gaithersburg, MD), coverslipped with MOWIOL 4-88 (Calbiochem, Lajolla, CA) and examined.
 155 For 3,3'-diaminobenzidine (DAB) immunohistochemistry sections were incubated in a solution of
 156 0,3% H₂O₂ in 0,01 M PBS, pH 7.4 for 15 minutes to inhibit the endogenous peroxidase, before the
 157 incubation with blocking buffer. Following primary antibody incubation sections were incubated
 158 with goat anti rabbit IgG biotinylated secondary antibody (1:350, Vector Laboratories, Burlingame,
 159 CA) or horse anti goat IgG biotinylated secondary antibody (1: 250, Vector Laboratories,
 160 Burlingame, CA) for 2h at RT. Sections were washed and incubated in avidin-biotin-peroxidase
 161 complex (Vectastain ABC kit; Vector Laboratories, Burlingame, CA) for 2h at RT. The reaction
 162 was developed with DAB Peroxidase Substrate Kit, 3,3'-diaminobenzidine (Vector laboratories,
 163 Burlingame, CA) for 3-5 minutes. Sections were mounted on TESPA (3-aminopropyl-
 164 triethoxysilan) treated slides and then counterstained with 1% cresyl violet acetate solution (1-2
 165 minutes exposure) and coverslipped with Neo-Mont 109016 (Merck, Darmstadt, Germany).

166

167 **3.3 Quantitative analyses**

168 Cell counting was performed using Neurolucida software (MicroBrightfield, Colchester, VT).

169 *Diameters of DCX+ objects* (see below, in Results) *in the external capsule and pericapsular*
170 *regions*: the average object diameter (orthogonal to main axis) has been measured for all the
171 clusters and groups of scattered cells in the external capsule, claustrum and amygdala of 3 adult
172 animals using the straight line tool of ImageJ program after a proper calibration, then reporting the
173 minimum and maximum length to obtain a size range.

174 *Density of DCX+ objects in the external capsule at neonatal and adult ages*: the number of DCX+
175 cell clusters and groups has been counted in the whole extension of the external capsule in 3 adult
176 and 3 newborn animals, using a serial step of 12 cryostat sections (480 μm ; 11 sections for the adult
177 and 10 for the newborn). The density was calculated as the total number of objects/area (mm^2). A 3-
178 D reconstruction aimed at further characterize the DCX+ clusters in the adult has been made in the
179 posterior part of the external capsule (24 serial cryostat sections, 40 μm thick, corresponding to 0,96
180 mm of white matter tissue).

181 *Cell density in the amygdala and claustrum at neonatal and adult ages*: the total number of DCX+
182 cells present within the two pericapsular regions have been counted in 3 adult and 3 newborn
183 animals (three slices corresponding to the anterior, middle and posterior part of each anatomical
184 structure have been considered). The density was calculated as the total number of cells/area (mm^2).

185 *Linear density of DCX+ neurons in the cerebral cortex at neonatal and adult ages*: the DCX+ cells
186 present in the cortical layer II have been counted within two brain levels (L2 and L3) and three
187 regions (the cingulate cortex and the medial margin of the suprasylvian gyrus in the neocortex; the
188 piriform cortex in the paleocortex; see Fig. 6), using three cryostat sections/level, in 3 adult and 3
189 newborn animals. The linear density was calculated as the total number of cells/the cortical tract
190 length (mm).

191 *Cell soma diameters of DCX+ cells:* the average cell soma diameter (orthogonal to main axis) has
192 been measured for 200 cells in the cortex, claustrum and amygdala of 3 adult animals using the
193 *straight line* tool of ImageJ program after a proper calibration, then reporting the minimum and
194 maximum length to obtain a size range.

195 *DCX+/BrdU+ double staining:* the percentage of double-stained cells has been calculated after
196 analyzing 200 cells in the cortex, claustrum, external capsule and amygdala of 3 newborn (number
197 of DCX+/BrdU+ cell out of DCX+, single-stained cells) and 3 adult animals (for each survival
198 time: 1, 2 and 4 months).

199 *DCX+/NeuN+ double staining:* the percentage of double-stained cells has been calculated after
200 analyzing 200 cells in the cortex, claustrum and amygdala of 3 adult animals (number of
201 DCX+/NeuN+ cells out of DCX+, single-stained cells).

202 *DCX+/Tbr1+ and DCX+/Sp8+ double staining:* the percentage of double-stained cells has been
203 calculated after analyzing 200 cells in the cortex, external capsule, claustrum and amygdala of 3
204 newborn animals (number of DCX+/Tbr1+ or DCX+/Sp8+ cells out of DCX+, single-stained
205 cells).

206 *Statistical Analysis:* all graphics and relative statistical analysis have been made using GraphPad
207 Prism 5 Software (La Jolla, CA, USA), and included unpaired (two-tailed) Student's t test
208 (comparing only two groups), and two-way ANOVAs. $p < 0.05$ was considered as statistically
209 significant. Data are expressed as averages \pm standard deviation (SD).

210

211 **3.4 Image acquisition and processing**

212 Images from immunofluorescence specimens were collected with Leica TCS SP5 (Leica
213 Microsystems, Wetzlar, Germany) confocal microscope. Images from DAB immunohistochemistry
214 were collected with eclipse 80i Nikon microscope (Nikon, Melville, NY) connected to a color CCD
215 Camera. Images were processed using Adobe Photoshop CS4 (Adobe Systems, San Jose, CA) and

216 ImageJ version 1.50b (Wayne Rasband, Research Services Branch, National Institute of Mental
217 Health, Bethesda, Maryland, USA). Only general adjustments to color, contrast, and brightness
218 were made. The 3D reconstruction in the external capsule was performed using Neurolucida
219 software (MicroBrightfield, Colchester, VT) by aligning 24 consecutive coronal sections starting
220 from the onset of the thalamus. The sections were previously immunoreacted for DCX, using DAB
221 peroxidase staining and counterstained with 1% cresyl violet acetate solution.

222

223

224 **Results**

225

226 **Distribution of DCX+ cells in the adult sheep brain**

227 After systematic screening of the whole adult sheep brain several populations of DCX+ cells were
228 detected at different locations (Fig. 2): i) newly generated neuroblasts/neuronal-like cells within the
229 SVZ and hippocampal neural stem cell niches, ii) neuronal-like cells in the superficial layers of the
230 cerebral cortex, and iii) groups of neuroblasts/neuronal-like cells in the external capsule and
231 surrounding grey matter (claustrum and amygdaloid nuclei). No DCX+ cells were detected in the
232 striatum/putamen. In addition to their different location, these DCX+ cells appeared to vary in their
233 morphology and spatial organization (Fig. 2B,C). Cells in the neurogenic zones typically appeared
234 as previously described (Brus et al., 2010; 2013b): single elongated, bipolar neuroblasts in the SVZ
235 adjacent to the lateral ventricle wall and at the lower aspect of the hippocampal dentate gyrus (Fig.
236 2D); these neurogenic regions were used as an internal control for detection of local cell division
237 markers (Ki-67 antigen) and newly generated neurons identifiable through injection of exogenous
238 markers (BrdU) and subsequent detection at different survival times.

239

240 *DCX+ cells in the cerebral cortex*

241 As previously described in some cortical areas of other mammals (reviewed in Bonfanti and
242 Nacher, 2012), DCX+ neuronal-like cells were detected in the cerebral cortex of the adult sheep
243 (Fig. 3). These cells were present in the superficial layers of most paleo- and neo-cortex (Figs. 3A
244 and 3B). They were further characterized in order to use them as a population of DCX+ cortical
245 neurons which has been already described in other species, here studied in sheep. In the cortical
246 cytoarchitecture the DCX+ neuronal-like cells were localized in the upper part of layer II (at the
247 limit with layer I), being present along the entire antero-posterior and dorso-ventral axis of the
248 brain. They appeared to be more abundant in the piriform cortex (paleocortex) with respect to
249 neocortex (Fig. 2B; see below for quantitative analysis). Two main morphological types falling into
250 two cell body size categories were identified: small cells, diameter 4-7 μm (type 1 cells), and large
251 cells, diameter 9-12 μm (type 2 cells; Fig. 3C,D). The large-sized cells frequently appeared as
252 pyramidal-like neurons (similar to the "principal cells" previously described in rats by Gomez-
253 Climent et al., 2008), whereas the small cells mostly showed a simpler, bipolar morphology (Fig.
254 3C,D). The principal cell type can be further split into two main patterns linked to soma shape and
255 dendritic complexity: those with oval-shaped cell body and poorly ramified apical dendrites (here
256 referred to as type 2a) and others with more developed apical dendrite arborization and basal
257 dendrites (here referred to as type 2b; Fig. 3C,D). Type 2 cells were far less abundant with respect
258 to type 1 cells (around 7%; Fig. 3D).

259

260 *DCX+ cells in the external capsule and surrounding regions*

261 Additional DCX+ cell populations were detectable in the external capsule and surrounding regions
262 (claustrum and amygdala). Most of these cells were grouped into discrete bulks to form either
263 tightly-packed cell clusters (mainly in the white matter; Fig. 2E), or groups of scattered cells (more
264 frequently observed in grey matter; Fig. 2G). Due to their heterogeneity, and in order to perform a
265 quantitative analysis, they were considered as "DCX+ objects", divided into compact cell clusters

(within the external capsule) and groups of scattered cells (in the surrounding regions: amygdala and claustrum).

External capsule. Most DCX⁺ cells in capsular white matter appeared as bipolar, elongated elements, often endowed with very long cell processes, assembled to form tightly-packed cell clusters (Fig. 4C). These clusters showed remarkable diameter variability (between 50 and 380 μ m). When observed in single coronal sections, some of them were reminiscent of the thick chains of neuroblasts described in the SVZ of rodents (Lois et al., 1996) and in the surrounding regions of rabbits (Luzzati et al., 2003; Ponti et al., 2006). Hence, a 3D reconstruction was performed through an anterior-posterior portion of the external capsule (Fig. 4B; see Methods) in order to assess their relationship with the SVZ neurogenic site. The analysis revealed that all clusters appear as discrete bulks of cells not forming long streams and never contacting the SVZ neurogenic site. In order to investigate the relationship with surrounding cells (e.g., the occurrence of specific astrocytic arrangements), immunocytochemistry for glial fibrillary astrocytic protein (GFAP) was performed. GFAP staining did not revealed any special density or niche-like organization adjacent to the DCX⁺ cells (Fig. 4D); yet, when the DCX⁺ cells were organized to form tightly-packed clusters they occupied glial-empty spaces, the astrocytes being segregated outside them (Fig. 4D). Quantification of DCX⁺ cell clusters (see below and Table 3) revealed that virtually all of them were contained within the external capsule, mostly residing in its posterior part (Fig. 4B). This analysis further excluded any direct contact between the clusters and the SVZ neurogenic site. Groups of less tightly-packed cells and scattered/isolated cells were also observed (Fig. 4C).

Amygdala and claustrum. Compact cell clusters were rare in the peri-capsular grey matter, whereas populations of scattered DCX⁺ cells were prevalent (Fig. 5). These cell groups were larger in the amygdala (diameter ranging between 125 and 385 μ m) than in claustrum (40 to 200 μ m). Within both regions, large multipolar DCX⁺ neurons endowed with long, dendritic-like processes were mixed with smaller, bipolar cells (Fig. 5B,C). Bipolar cells represented by large the most frequent cell morphology (around 98-99%; Fig. 5D). Three main cell morphologies were present in the

292 amygdala (Fig. 5B): type 1 cells (small, bipolar; soma diameter 3-6 μm), type 2 cells (medium-
293 sized, similar to type 2a cells in cortex; soma diameter 8-9 μm), and type 3 cells (large, multipolar;
294 soma diameter 9-11 μm). Two main cell types were detectable in the claustrum (Fig. 5C): type 1
295 cells (small, unipolar or bipolar; soma diameter 3-6 μm), type 2 cells (soma diameter 7-9 μm).

296

297 **DCX+ cell populations at different ages**

298 The same types of analyses performed on the DCX+ cells in the cortex, capsular and pericapsular
299 regions were carried out on early postnatal brains (7 days after birth). Under a qualitative profile, by
300 comparing the occurrence and distribution of DCX+ cell populations at different ages, the only
301 substantial difference concerned the presence of cell clusters within the putamen of the newborn
302 and within the corpus callosum of neonatal and prepuberal animals (not shown), both cell
303 populations then disappearing in adults (article in preparation). All other DCX+ cell populations,
304 including cortical immature neurons, neuroblasts of the neurogenic sites, and DCX+ cells in
305 capsular/pericapsular regions were present at both ages. Yet, quantitative evaluations carried out in
306 neonates and adults revealed differences among these regions (Fig. 6). When compared to
307 newborns, the cerebral cortex of adult animals showed an evident and generalized decrease in the
308 amount of DCX+ immature neurons (Fig. 6A, top). To quantify this reduction we calculated the
309 linear density of layer II DCX+ cells in three cortical segments, including both neocortex and
310 paleocortex of neonatal and adult sheep (see Methods and Fig. 6A, bottom). In all analyzed regions
311 both the number and density of DCX+ cells underwent approximately a four-fold reduction with
312 age (see Table 3 for statistical comparisons). Such trend, suggesting an age-related reduction in
313 cortical plasticity of the layer II (as previously shown in several species; Abrous et al., 1997; Varea
314 et al., 2009), parallels the remarkable drop described for the DCX+ cell populations in the
315 neurogenic sites of different mammals (Sanai et al., 2011; Lipp and Bonfanti, 2016) which is also
316 strikingly evident in both SVZ and hippocampus of sheep (Fig. 6B).

317 Interestingly enough, in contrast with their neocortical counterparts, both the number and the
318 density of DCX+ cell populations in the capsular and pericapsular regions were substantially stable
319 at both ages (Fig. 6C and Table 3 for statistics). The slight reduction in the density of DCX+ cell
320 clusters detectable in the external capsule is related to the relative increase in the area of this region
321 with respect to others (increasing volume of the capsule itself; see Table 3). Two way ANOVA
322 analyses confirmed the presence of a significant interaction between brain region and age for both
323 number ($F=136,551$; $p<0.0001$) and density of DCX+ cells/objects ($F=84,258$; $p<0.0001$). Pairwise
324 comparisons clearly showed that subcortical regions had a similar age related trend that differed
325 from that of both paleo and neocortex (Table 3). As to the topographical localization of the DCX+
326 objects within each brain region, these structures were located more posteriorly in the adult external
327 capsule, whereas in the newborn they were distributed homogeneously along the entire antero-
328 posterior axis. In claustrum and amygdala the distribution was generally homogeneous (in the latter,
329 mainly located in the basolateral nucleus).

330

331 **Cell proliferation analysis**

332 The heavy occurrence of DCX+ cells in the cerebral cortex, external capsule and surrounding
333 regions of the sheep brain opens the question whether they are newly generated. Analysis with Ki-
334 67 antigen and BrdU in adults consistently revealed immunopositive nuclei in both SVZ and
335 hippocampal neurogenic sites, here used as internal controls for detection of cell proliferation
336 markers and neurogenesis (see Fig. 2). By contrast, no Ki-67/DCX colocalization was detectable in
337 all cortical, capsular/pericapsular regions analyzed (Fig. 7A), as well as no BrdU staining were
338 found in association with parenchymal DCX+ cells in any of the adult animals injected with the
339 exogenous cell proliferation marker and subsequently analysed at 30, 60, 120 days survival (Fig.
340 7A). The results obtained by joining local cell proliferation marker and BrdU pulse labelling

analyses strongly indicate that the external capsule/pericapsular DCX+ cells are not dividing at any of the adult ages considered, thus excluding the occurrence of parenchymal neurogenesis. To confirm that these cell populations were generated earlier, during embryogenesis, DCX/BrdU double staining was performed in lambs born from mothers injected with BrdU 3 months before parturition (Fig. 7B). Numerous BrdU+ nuclei were consistently present in all areas analysed. In the external capsule of neonates, some of them were detectable in DCX+ cells of the tightly-packed clusters as well as in isolated cells (Fig. 7B). Some BrdU+ cells were DCX-negative, likely corresponding to post-mitotic (mature) neurons which had been generated during embryogenesis and having already lost their DCX staining (see below). DCX+ cells not immunoreactive for BrdU were also present, indicating immature cells generated at previous or later developmental stages. After analysis with Ki-67 antigen in neonates, some scattered immunopositive nuclei were detectable at different locations of the brain parenchyma, yet never involving double-staining with DCX+ cells (Fig. 7B), thus indicating that these latter are no more proliferating after birth. A similar pattern was observed in the cortex where no Ki-67+/DCX+ or BrdU/DCX+ cells were detectable in the adult, whereas BrdU+/DCX+ cells were systematically detected in cortical layer II of neonates; these cells were far more abundant in the neocortex with respect to the paleocortex (see pie charts in Fig. 7B). Similarly to what observed in capsular/pericapsular regions, some Ki-67+ nuclei were present in the cortex of neonates but never in double staining with DCX.

Cell maturity/immaturity and pallial/subpallial origin markers

In order to get some insight concerning the degree of maturation of the DCX+ cell populations described here, we used markers commonly employed to assess their neuronal maturational stage. We analysed NeuN, an RNA-binding protein expressed by most postmitotic neurons which start differentiation (Mullen et al., 1992; Fig. 8A). Only a small percentage of the DCX+ cells (around 10%) co-expressed NeuN in different regions (11,7% in cortical layer II; 9,1% in claustrum; 8,3%

366 in amygdala; Fig. 8B). In the cortex, all the DCX+/NeuN+ neurons fell in the type 2 cell
367 morphology with ramified dendrites. In the external capsule NeuN was not detectable within the
368 tightly-packed cell clusters, whereas some isolated cells detached from the clusters were double-
369 stained (Fig. 8A). This gives support to the hypothesis that larger DCX+ cells in layer II are slightly
370 more mature than small cells, showing increases in NeuN expression as described during neuronal
371 differentiation in the adult dentate gyrus (Kempermann et al., 2004; Marques-Mari et al., 2007).
372 Similarly, another marker of mature neuronal cells (HuC/D RNA-binding protein; Barami et al.,
373 1995) was detected only in some of the cortical DCX+ neurons (again, mostly large, type 2 cells;
374 Fig. 8C). In parallel, subpopulations of DCX+ cells in all regions investigated were immunoreactive
375 for PSA-NCAM, a marker of immaturity expressed by cells retaining plasticity (Bonfanti, 2006).
376 Unlike newly generated neuroblasts of the classic neurogenic sites (SVZ and dentate gyrus) which
377 are mostly PSA-NCAM immunoreactive, in cortex, amygdala, claustrum and external capsule the
378 staining was detectable only in some DCX+ cells, being restricted to parts of their membrane (Fig.
379 8D). A similar pattern was observed with the A3 subunit of the cyclic nucleotide-gated ion channel
380 (CNGA3; Fig. 8E), which has been previously shown in immature cortical neurons (Varea et al.,
381 2011) and is considered involved in brain plasticity (Michalakis et al., 2011). The results obtained
382 with the above mentioned markers were substantially similar in all regions and ages considered. On
383 the whole, many DCX+ cells (of both types) also expressed markers of immaturity whereas only
384 small subpopulations (NeuN, mainly type 2 cells) or a few of them (HUC/D) expressed markers of
385 differentiation/maturity (summarized in Fig. 8F).

386 Once assessed the prenatal origin of the parenchymal DCX+ cells, the embryologic divisions
387 (neural progenitor domains) of their origin were investigated by employing two markers of pallial
388 (T-box transcription factor, *Tbr1*) and subpallial origin (zinc-finger protein, *Sp8*; experiments
389 carried out on neonates). The presence of these two proteins was analyzed in the various areas
390 investigated. As previously reported in other mammals, *Tbr1* was present in pallial derivatives such
391 as the hippocampus, claustrum, amygdala, and piriform cortex, being frequently associated with the

392 DCX+ neurons (Fig. 9). In the neocortex, *Tbr1* was strongly expressed in deeper layers with respect
393 to upper layers (where it was mainly found in type 1 cells of the layer II; Fig. 9A). Interestingly, in
394 cortical upper layers this transcription factor is downregulated during neuronal maturation, at least
395 in mice (Toma et al. 2014). Only rare cells were positive for *Sp8* in these two regions (2,2% in
396 cortex and 1,4% in claustrum). By contrast, the situation was more heterogeneous in the external
397 capsule and amygdala: two intermixed but distinct cell populations were immunopositive for each
398 one of the two markers, with a prevalence of *Tbr1*+ cells (Fig. 9B). These results strongly support
399 the view that the DCX+ immature cells in subcortical regions are generated from both subpallial
400 and pallial regions (about 25% and 75%, respectively) of the embryonic SVZ.

401

402

403 Discussion

404

405 The cytoskeletal protein DCX is associated with neuronal maturation and cell shape global
406 remodeling, thus being involved in structural plasticity (Nacher et al., 2001; Brown et al., 2003).
407 For decades, much attention has been drawn on adult neurogenesis as a striking process of plasticity
408 involving the production of new neurons which impact on learning and memory, also opening
409 possibilities for brain repair (Martino et al., 2011; Peretto and Bonfanti, 2014; Berninger and
410 Jessberger, 2016). In mammals, the functional integration of newborn neurons is highly restricted to
411 olfactory bulb and hippocampus (Bonfanti and Peretto, 2011), their stem cell niches being less
412 active in humans than in rodents (Sanai et al., 2011; Lipp and Bonfanti, 2016). An emerging form of
413 plasticity consists of cells retaining features of immaturity through adulthood, including the
414 persistent expression of DCX though they are not generated *de novo* postnatally ("immature
415 neurons", Gomez-Climent et al., 2008). Originally, these cells were described in the paleocortex of
416 rodents (Seki and Arai, 1991; Bonfanti et al., 1992). Their distribution and role remain largely

417 object of investigation, systematic studies being scarce (Bonfanti and Nacher, 2012; König et al.,
 418 2016). In some mammals, similar cells are also present in neocortex (Xiong et al., 2008; Cai et al.,
 419 2009; Luzzati et al., 2009; Zhang et al., 2009), leading to speculate that non-neurogenic structural
 420 plasticity might be prominent in non-rodent species (Bonfanti, 2016 and present work).
 421 We screened the occurrence, location, distribution and developmental origin of DCX⁺ cells as an
 422 indicator of non-neurogenic plasticity in sheep: long-living mammals endowed with relatively
 423 large-sized, gyrencephalic brain. By using markers of cell division (Ki-67) and pulse labelling of
 424 BrdU, we revealed the presence of abundant DCX⁺ cell populations born prenatally and not
 425 generated after birth. These cells were not restricted to cerebral cortex, also occurring in white and
 426 grey matter of pallial subcortical regions: external capsule, claustrum, amygdala. In contrast with
 427 the substantial decrease in number of DCX⁺ cortical neurons at increasing ages (Abrous et al.,
 428 1997; Xiong et al., 2008; Cai et al., 2009; Varea et al., 2009, here confirmed in sheep), the
 429 subcortical DCX⁺ cells appear steadily maintained through time, at least in young adults (Figs. 6
 430 and 10). Groups of DCX⁺ cells were previously found close to the external capsule in rabbits
 431 (Luzzati et al., 2003) and in the amygdala of non-human primates (Zhang et al., 2009; de Campo et
 432 al., 2012). A small portion of them were considered as newly generated in the amygdala of rabbits
 433 (Luzzati et al., 2003), mouse (Jhaveri et al., 2017) and primates (Bernier et al., 2002). Our
 434 experiments in the sheep excluded the occurrence of adult newborn neurons in any of the
 435 parenchymal regions containing DCX⁺ cells, thus revealing species-specific heterogeneity in their
 436 regional distribution.
 437 As to the maturational stage of the cells, many of them expressed the markers of
 438 immaturity/plasticity PSA-NCAM and CNGA3, in addition to DCX. Also the *Tbr1* expression in
 439 DCX⁺ cortical cells (mainly of type 1) in layer II (wherein the transcription factor is usually
 440 downregulated with maturation; see Toma et al., 2014) further supports their immature state. On the
 441 other hand, the vast majority (around 90%) did not express NeuN, a soluble nuclear protein whose
 442 immunoreactivity becomes obvious as neurons are initiating cellular differentiation (Mullen et al.,

443 1992), and only a few of them did express HuC/D. The small percentage of DCX+ cells which
 444 express markers of differentiation/maturity (mainly those with complex morphology) are likely in a
 445 state ready for further differentiation. Notably, in cortex and amygdala their morphology is
 446 reminiscent of the principal cell type (Washburn and Moises, 1992). Hence, most of the DCX+ cells
 447 appear to be in an intermediate state of immaturity (Fig. 8F). Theoretically, they may either be adult
 448 “immature neurons” in standby mode, or adult neurons undergoing structural plasticity (i.e., a “de-
 449 maturation and re-maturation” process akin to dedifferentiation and redifferentiation). Due to
 450 obvious difficulties in performing functional experimental tests in sheep, these latter options remain
 451 hypothetical. Yet, these results, including the fact that immature cell populations in subcortical
 452 regions appear more stable over time with respect to their cortical counterpart, open new
 453 possibilities for the existence of unusual/unknown forms of plasticity in multiple brain regions of
 454 non-rodent mammals. The fact that “immature” cell populations in the sheep brain are not
 455 regionally restricted as they are in rodents, confirms that non-neurogenic structural plasticity might
 456 be higher in non-rodent species (Bonfanti and Nacher, 2012; Fig. 10). Since adult neurogenesis is
 457 well preserved in rodents and highly reduced in species evolutionarily and structurally closer to
 458 humans (Sanai et al., 2011; Paredes et al., 2015; Parolisi et al., 2015,2017; Lipp and Bonfanti,
 459 2016), we suggest that non-neurogenic plasticity might have been preserved better in long-living,
 460 large-brained mammals (though only studies through mammalian orders might identify putative
 461 phylogenetic trends).

462 Markers of pallial/subpallial origin were used to get insights into the embryologic origin and, to a
 463 lesser extent, the possible fate of the DCX+ cells described here. According to the tetrapartite model
 464 of pallial subdivision in vertebrate brain, four main territories of progenitor domains can be
 465 recognized in pallial germinative regions: medial, dorsal, lateral, ventral pallium (Holmgren, 1925;
 466 Puelles et al., 2000). *Tbr1* is a neuron specific, post-mitotic transcription factor mostly found in
 467 pallium-derived neurons committed to differentiate into excitatory glutamatergic neurons (Bedogni
 468 et al., 2010; Puelles et al., 2000, McKenna et al., 2011). Most of the DCX+ cells described here in

cortical and subcortical regions expressed *Tbr1*, thus belonging to the glutamatergic principal cortical cells of pallial origin (Hevner et al., 2001). Whereas in rodents the DCX+ immature neurons are confined in the ventral pallial derivative (paleocortex), we show that immature neurons in sheep extend into other ventral (amygdala), dorsal (neocortex) and lateral (claustrum) pallial derivatives. In the external capsule and amygdala, part of the DCX+ cells expressed *Sp8*, a transcription factor marking specific populations of olfactory bulb interneurons, strongly expressed in the dorsal lateral ganglionic eminence (a subpallium domain; Waclaw et al., 2006) and in one-fifth of adult cortical interneurons (Ma et al., 2011). We show that the vast majority of DCX+ cortical and claustrum neurons in sheep are of pallial origin, whereas capsular and amygdalar DCX+ cells are of mixed origin (pallial and non-pallial sources). Hence, it is very likely that capsular and peri-capsular immature neurons derive from different populations during embryogenesis, though genetic lineage tracing would be required to confirm this. Since the anlage of the external capsule is a migration route for *Tbr1*+ and *Sp8*+ cells directed to claustrum and amygdala (Waclaw et al., 2006; Puelles et al., 2017), the DCX+ cells in subcortical regions might represent a remnant of immature cells remaining in the white matter during postnatal brain growth. As to the possible function of the DCX+ "immature" neurons, no substantial insight have been obtained until now, even in rodents. In the rat paleocortex they are considered as a reservoir of undifferentiated elements somehow kept in a "stand by" mode (Gomez-Climent et al., 2008). The current hypothesis (utterly theoretical), is that they might lose immaturity at a certain point of life, possibly integrating in the neural circuits by accomplishing their differentiation (Bonfanti and Nacher, 2012). In brain regions hosting adult neurogenesis (olfactory bulb, hippocampus), young neurons are endowed with special plastic properties enabling them to substantially affect neural functions independently from their long-term integration (Stone et al., 2011; Ishikawa et al., 2014). Thus, an intriguing possibility is that, in some mammals, other pallial regions may foster related types of plasticity by extending the immature phase of specific neuronal subpopulations without the need of increasing their number. In the cortex, immature *Tbr1*/DCX+ neurons gradually fade-off

495 during post-natal life (Abrous et al., 1997; Xiong et al., 2008; Cai et al., 2009; this study)
496 suggesting that they could be related to cortical maturation. The reason why the number of DCX+
497 cells in claustrum and amygdala remain strikingly constant during post-natal stages is puzzling.
498 These cells may represent a specific subpopulation that constitutively express DCX through life and
499 support a form of plasticity that is independent from the general trend of maturation-related
500 structural plasticity. All brain structures hosting the DCX+ immature neurons mediate high
501 cognitive functions, including learning, memory and emotional activities. The amygdala has an
502 essential role in the formation of emotion-related memories (LaBar and Phelps, 1998), whereas the
503 claustrum is considered important in consciousness (Crick and Koch, 2005). Finally, an important
504 point will be to understand the evolutionary relationships of the DCX+ cells. *Tbr1*+ /DCX+ cells are
505 present in pallial derivatives of reptiles (including the dorsal ventricular ridge, a ventral pallial
506 derivative homologous of the amygdala; Puelles et al., 2017), leading to propose that they could
507 represent a conserved pallial cell type (Luzzati, 2015). Collectively, these observations support the
508 possibility that a population of slowly maturing DCX+ cells might be shared by multiple pallial
509 domains being conserved during evolution despite the profound functional/anatomical changes.
510 Independently from any specific function, “immature” neurons raise interest in the general context
511 of mammalian structural plasticity, representing an endogenous reserve of potentially plastic cells.

521

522

523

524 **References**

525

526 Abrous DN, Montaron MF, Petry KG, Rougon G, Darnaudery M, Le Moal M, Mayo W (1997)
527 Decrease in highly polysialylated neuronal cell adhesion molecules and in spatial learning during
528 ageing are not correlated. *Brain Res* 744, 285-292.

529

530 Aimone JB, Li Y, Lee SW, Clemenson GD, Deng W, Gage FH (2014) Regulation and function of
531 adult neurogenesis: from genes to cognition. *Physiol Rev* 94, 1991-1026.

532

533 Bailey CH, Kandel ER, Harris KM (2015) Structural components of synaptic plasticity and memory
534 consolidation. *Cold Spring Harb Perspect Biol.* 7: a021758.

535

536 Barami K, Iversen K, Furneaux H, Goldman SA (1995) Hu protein as an early marker of neuronal
537 phenotypic differentiation by subependymal zone cells of the adult songbird forebrain. *J Neurobiol*
538 28: 82-101.

539

540 Bedogni F, Hodge RD, Elsen GE, Nelson BR, Daza RA, Beyer RP, Bammler TK, Rubenstein JL,
541 Hevner RF (2010) Tbr1 regulates regional and laminar identity of postmitotic neurons in
542 developing neocortex. *Proc Natl Acad Sci USA* 107: 13129-13134.

543

544 Bernier P J, Bedard A, Vinet J, Levesque M, Parent A (2002) Newly generated neurons in the
545 amygdala and adjoining cortex of adult primates. *Proc Natl Acad Sci USA* 99, 11464-11469.

546

547 Berninger B, Jessberger S (2016) Engineering of adult neurogenesis and gliogenesis. Cold Spring
548 Harb Perspect Biol 8(5) pii: a018861.

549

550 Beul SF, Hilgetag CC (2015) Towards a “canonical” agranular cortical microcircuit. Front
551 Neuroanat 8:165.

552

553 Bonfanti L (2006) PSA-NCAM in mammalian structural plasticity and neurogenesis. Prog
554 Neurobiol 80:129-164.

555

556 Bonfanti L (2016) Adult neurogenesis 50 years later: Limits and opportunities in mammals. Front
557 Neurosci 10:44.

558

559 Bonfanti L, Olive S, Poulain DA, Theodosis DT (1992) Mapping of the distribution of
560 polysialylated neural cell adhesion molecule throughout the central nervous system of the adult rat:
561 an immunohistochemical study. Neuroscience 49: 419-436.

562

563 Bonfanti L, Nacher J (2012) New scenarios for neuronal structural plasticity in non-neurogenic
564 brain parenchyma: the case of cortical layer II immature neurons. Prog Neurobiol 98: 1-15.

565

566 Bonfanti L, Peretto P (2011) Adult neurogenesis in mammals -a theme with many variations. Eur J
567 Neurosci 34: 930-950.

568

569 Bonfanti L, Theodosis DT (2009) Polysialic acid and activity-dependent synapse remodeling. Cell
570 Adhes Migrat 3: 43-50.

571

572 Brown JP, Couillard-Despres S, Cooper-Kuhn CM, Winkler J, Aigner L, Kuhn HG (2003)
573 Transient expression of doublecortin during adult neurogenesis. *J Comp Neurol* 467: 1-10.
574

575 Brus M, Meurisse M, Franceschini I, Keller M, Levy F (2010) Evidence for cell proliferation in the
576 sheep brain and its down-regulation by parturition and interactions with the young. *Horm Behav* 58:
577 737-746.
578

579 Brus M, Keller M, Lévy F (2013a) Temporal features of adult neurogenesis: differences and
580 similarities across mammalian species. *Front Neurosci* 7:135-144.
581

582 Brus M, Meurisse M, Gheusi G, Keller M, Lledo P, Levy F (2013b) Dynamics of olfactory and
583 hippocampal neurogenesis in adult sheep. *J Comp Neurol* 521: 169-188
584

585 Cai Y, Xiong K, Chu Y, Luo DW, Luo XG, Yuan XY, Struble RG, Clough RW, Spencer DD,
586 Williamson A, Kordower JH, Patrylo PR, Yan XX (2009) Doublecortin expression in adult cat and
587 primate cerebral cortex relates to immature neurons that develop into GABAergic subgroups. *Exp*
588 *Neurol* 216: 342-356.
589

590 Crick FC, Koch C (2005) What is the function of the claustrum? *Phil Trans R Soc B* 360, 1271-
591 1279.
592

593 de Campo DM, Fudge JL (2012) Where and what is the paralaminar nucleus? A review on a unique
594 and frequently overlooked area of the primate amygdala. *Neurosci Biobehav Rev* 36: 520-535.
595

596 Feliciano DM, Bordey A, Bonfanti L (2015) Noncanonical Sites of Adult Neurogenesis in the
597 Mammalian Brain. *Cold Spring Harb Perspect Biol* 7:a018846.

598

599 Frotscher M (1992) Specificity of interneuronal connections. *Ann Anat* 174: 377-382.

600

601 Gleeson JG, Lin PT, Flanagan LA, Walsh CA (1999) Doublecortin is a microtubule-associated
602 protein and is expressed widely by migrating neurons. *Neuron* 23:257–271. doi: 10.1016/S0896-
603 6273(00)80778-3

604

605 Gómez-Climent MA, Castillo-Gómez E, Varea E, Guirado R, Blasco-Ibáñez JM, Crespo C,
606 Martínez-Guijarro FJ, Nacher J (2008) A population of prenatally generated cells in the rat
607 paleocortex maintains an immature neuronal phenotype into adulthood. *Cereb Cortex* 18: 2229-
608 2240.

609

610 Grandel H, Brand M (2013) Comparative aspects of adult neural stem cell activity in vertebrates.
611 *Dev Genes Evol* 223:131-47.

612

613 Hevner RF, Shi L, Justice N, Hsueh Y, Sheng M, Smiga S, Bulfone A, Goffinet AM, Campagnoni
614 AT, Rubenstein JL (2001) Tbr1 regulates differentiation of the preplate and layer 6. *Neuron* 29: 353-
615 366.

616

617 Holmgren N (1925) Points of view concerning forebrain morphology in higher vertebrates. *Acta*
618 *Zool Stockh* 6: 413-477.

619

620 Ishikawa R, Kim R, Namba T, Kohsaka S, Uchino S, Kida S (2014) Time-dependent enhancement
621 of hippocampus-dependent memory after treatment with memantine: Implications for enhanced
622 hippocampal adult neurogenesis. *Hippocampus* 24(7):784-793.

623

624 Jhaveri DJ, Tedoldi A, Hunt S, Sullivan R, Watts NR, Power JM, Bartlett PF, Sah P (2017)
625 Evidence for newly generated interneurons in the basolateral amygdala of adult mice. *Mol Psych*
626 (E-pub) doi: 10.1038/mp.2017.134.

627

628 Kempermann G, Jessberger S, Steiner B, Kronenberg G (2004) Milestones of neuronal development
629 in the adult hippocampus. *Trends Neurosci* 27, 447-452.

630

631 König R, Benedetti B, Rotheneichner P, O'Sullivan A, Kreutzer C, Belles M, Nacher J, Weiger TM,
632 Aigner L, Couillard-Després S (2016) Distribution and fate of DCX/PSA-NCAM expressing cells
633 in the adult mammalian cortex: A local reservoir for adult cortical neuroplasticity? *Front Biol* 11:
634 193-213.

635

636 LaBar KS, Phelps EA (1998) Role of the human amygdala in arousal mediated memory
637 consolidation. *Psych Sci* 9:490-493.

638

639 Lipp HP, Bonfanti L (2016) Adult neurogenesis in mammals: variations and confusions. *Brain*
640 *Behav Evol* 87:205-221.

641

642 Lois C, García-Verdugo JM, Alvarez-Buylla A (1996) Chain migration of neuronal precursors.
643 *Science* 271:978-981.

644

645 Luzzati F, Peretto P, Aimar P, Ponti G, Fasolo A, Bonfanti L (2003) Glia-independent chains of
646 neuroblasts through the subcortical parenchyma of the adult rabbit brain. *Proc Natl Acad Sci USA*
647 100:13036-13041.

648

649 Luzzati F, Bonfanti L, Fasolo A, Peretto P (2009) DCX and PSA-NCAM expression identifies a
650 population of neurons preferentially distributed in associative areas of different pallial derivatives
651 and vertebrate species. *Cereb Cortex* 19:1028-41.

652

653 Luzzati F (2015) A hypothesis for the evolution of the upper layers of the neocortex through co-
654 option of the olfactory cortex developmental program. *Front Neurosci* 12;9:162.

655

656 Ma T, Zhang Q, Cai Y, You Y, Rubenstein JLR, Yang Z (2011) A subpopulation of dorsal
657 lateral/caudal ganglionic eminence-derived neocortical interneurons expresses the transcription
658 factor Sp8. *Cereb Cortex* 22: 2120-2130.

659

660 Marques-Mari AI, Nacher J, Crespo C, Gutierrez-Mecinas M, Martinez-Guijarro FJ, Blasco-Ibanez,
661 JM (2007) Loss of input from the mossy cells blocks maturation of newly generated granule cells.
662 *Hippocampus* 17, 510-524.

663

664 Martino G, Pluchino S, Bonfanti L, Schwartz M (2011) Brain regeneration in physiology and
665 pathology: the immune signature driving therapeutic plasticity of neural stem cells. *Physiol Rev*
666 91:1281-304.

667

668 McKenna WL, Betancourt J, Larkin KA, Abrams B, Guo C, Rubenstein JL, Chen B (2011) Tbr1
669 and Fezf2 regulate alternate corticofugal neuronal identities during neocortical development. *J*
670 *Neurosci* 31: 549-564.

671

672 Michalakakis S, Kleppisch T, Polta SA, Wotjak CT, Koch S, Rammes G, Matt L, Becirovic E, Biel M
673 (2011) Altered synaptic plasticity and behavioral abnormalities in CNGA3-deficient mice. *Genes*
674 *Brain Behav* 10: 137-148.

675

676 Mullen RJ, Buck CR, Smith AM (1992) NeuN, a neuronal specific nuclear protein in vertebrates.
677 Development 116: 201-211.

678

679 Nacher J, Crespo C, McEwen BS (2001) Doublecortin expression in the adult rat telencephalon.
680 European J Neurosci 14: 629-644.

681

682 Nacher J, Bonfanti L (2015) New neurons from old beliefs in the adult piriform cortex? A
683 Commentary on: "Occurrence of new neurons in the piriform cortex". Front Neuroanat 9: 62.

684

685 Paredes MF, Sorrells SF, Garcia-Verdugo JM, Alvarez-Buylla A (2015) Brain size and limits to
686 adult neurogenesis. J Comp Neurol 524:646-64.

687

688 Parolisi R, Peruffo A, Messina S, Panin M, Montelli S, Giurisato M, Cozzi B, Bonfanti L (2015)
689 Forebrain neuroanatomy of the neonatal and juvenile dolphin (*T. truncatus* and *S. coeruleoalba*).
690 Front Neuroanat. 9: 140.

691

692 Parolisi R, Cozzi B, Bonfanti L (2017) Non-neurogenic SVZ-like niche in dolphins, mammals
693 devoid of olfaction. Brain Struct Funct 222: 2625-2639.

694

695 Peretto P, Bonfanti L (2014) Major unsolved points in adult neurogenesis: doors open on a
696 translational future? Front Neurosci 8:154.

697

698 Ponti G, Aimar P, Bonfanti L (2006) Cellular composition and cytoarchitecture of the rabbit
699 subventricular zone (SVZ) and its extensions in the forebrain. J Comp Neurol 498:491-507.

700

701 Puelles, L, Kuwana E, Puelles E, Bulfone A, Shimamura K, Keleher J, Smiga S, Rubenstein JLR
 702 (2000) Pallial and subpallial derivatives in the embryonic chick and mouse telencephalon, traced by
 703 the expression of the genes *Dlx-2*, *Emx-1*, *Nkx-2.1*, *Pax-6*, and *Tbr-1*. J Comp Neurol 424: 409-438.
 704
 705 Puelles L, Sandoval JE, Ayad A, del Corral R, Alonso A, Ferran JL, Martinez-de-la-Torre M (2017)
 706 The pallium in reptiles and birds in the light of the updated tetrapartite pallium model. In Jon H
 707 Kaas Ed., Evolution of Nervous Systems, 2nd edition, Vol. 1 Elsevier.
 708
 709 Sanai N, Nguyen T, Ihrie RA, Mirzadeh Z, Tsai H-H, Wong M, Gupta N, Berger MS, Huang E,
 710 Garcia-Verdugo JM, Rowitch DH, Alvarez-Buylla A (2011) Corridors of migrating neurons in the
 711 human brain and their decline during infancy. Nature 478: 382-386.
 712
 713 Seki T, Arai Y (1991) Expression of highly polysialylated NCAM in the neocortex and piriform
 714 cortex of the developing and the adult rat. Anat Embryol (Berl.) 184: 395-401.
 715
 716 Spalding KL, Bergmann O, Alkass K, Bernard S, Salehpour M, Huttner HB, Bostrom E,
 717 Westerlund I, Vial C, Buchholz BA, Possnert G, Mash DC, Druid H, Frisen J (2013) Dynamics of
 718 hippocampal neurogenesis in adult humans. Cell 153:1219-1227.
 719
 720 Stone SS, Teixeira CM, Zaslavsky K, Wheeler AL, Martinez-Canabal A, Wang AH, Sakaguchi M,
 721 Lozano AM, Frankland PW (2011) Functional convergence of developmentally and adult-generated
 722 granule cells in dentate gyrus circuits supporting hippocampus-dependent memory. Hippocampus
 723 21(12):1348-1362.
 724
 725 Theodosis DT, Poulain DA, Olier SH (2008) Activity-dependent structural and functional plasticity
 726 of astrocyte-neuron interactions. Physiol Rev 88:983-1008. doi: 10.1152/physrev.00036.2007

727

728 Toma K, Kumamoto T, Hanashima C (2014) The timing of upper-layer neurogenesis is conferred
729 by sequential derepression and negative feed back from deep-layer neurons. *J Neurosci* 34: 13259-
730 13276.

731

732 Varea E, Castillo-Gomez E, Gomez-Climent MA, Guirado R, Blasco-Ibanez JM, Crespo C,
733 Martinez-Guijarro FJ, Nacher J (2009) Differential evolution of PSANCAM expression during
734 aging of the rat telencephalon. *Neurobiol Aging* 5, 808-818.

735

736 Varea E, Belles M, Vidueira S, Blasco-Ibáñez JM, Crespo C, Pastor AM, Nacher J (2011) PSA-
737 NCAM is expressed in immature, but not recently generated, neurons in the adult cat cerebral
738 cortex layer II. *Front Neurosci* 5: 17.

739

740 Wacław RR, Allen ZJ 2nd, Bell SM, Erdélyi F, Szabó G, Potter SS, Campbell K (2006) The zinc
741 finger transcription factor Sp8 regulates the generation and diversity of olfactory bulb interneurons.
742 *Neuron* 49: 503-516.

743

744 Wacław RR, Ehrman LA, Pierani A, Campbell K (2010) Developmental origin of the neuronal
745 subtypes that comprise the amygdalar fear circuit in the mouse. *J Neurosci* 30:6944-6953.

746

747 Washburn MS, Moises HC (1992) Electrophysiological and morphological properties of rat
748 basolateral amygdaloid neurons in vitro. *J Neurosci* 12: 4066-4079.

749

750 Xiong K, Luo D-W, Patrylo PP, Luo X-G, Struble RG, Clough RW, Yan X-X (2008) Doublecortin-
751 expressing cells are present in layer II across the adult guinea pig cerebral cortex: Partial
752 colocalization with mature interneuron markers. *Exp Neurol* 211:271-282.

753

754 Zhang X-M, Cai Y, Chu Y, Chen E-Y, Feng J-C, Luo X-G, Xiong K, Struble RG, Clough RW,
755 Patrylo PR, Kordower JH, Yan X-X (2009) Doublecortin-expressing cells persist in the associative
756 cerebral cortex and amygdala in aged nonhuman primates. *Front Neuroanat* 3: 17.

757

758

Figure legends

Figure 1. A, Four levels of interest (L1-L4) in the whole sheep brain, obtained by re-drawing the Atlas of Brain Biodiversity Bank (Michigan State University; www.msu.edu) and adapted to our cryostat sections; the whole extension of the brain analysed is comprised between the arrowheads (dotted line). B, By combining levels L2 and L3, an additional, "ideal" level containing the most important neuroanatomical structures analyzed here was obtained (asterisk); this ideal level was used to represent Results. This representation refers to adult animals, yet no significant morphological/neuroanatomical differences were observed in younger animals. Nc, neocortex; Pc, paleocortex; Ic, internal capsule; Ec, external capsule; Ex, capsula extrema; Cl, claustrum; Am, amygdala; Pu, putamen; Cn, caudate nucleus; Lv, lateral ventricle; Cc, corpus callosum.

Figure 2. DCX+ cells in the adult sheep brain. A and C, representative level of the brain showing different locations of the DCX+ cells. B, main types of DCX+ cells encountered in our analysis (DCX+ "objects"), classified according to their morphology, spatial organization, and cell division history (newly born Vs. non-newly generated). D, newly generated neuroblasts in the SVZ and dentate gyrus (SGZ); in both neurogenic sites, DCX+ cells are intermingled with several nuclei immunoreactive for Ki-67 antigen (rarely double-stained in the SVZ due to different expression time-course of the markers); BrdU injected 60 days before sacrifice is detectable in DCX+ neuroblasts of the olfactory bulb (OB) and in hippocampal granule cells. E-G, representative photographs of the DCX+ cells/cell populations at the different locations showed in C: E, clusters of DCX+ cells in the external capsule (Ec); F, layer II cortical neurons; G, scattered DCX+ cells in the amygdala (Amy) and claustrum (Cl); Ex, capsula extrema. Scale bars: 30 μ m; D (bottom right), 20 μ m.

Figure 3. DCX+ cells in the cerebral cortex of adult sheep. A, Location of DCX+ neurons in the cortical layer II. Top, DCX (brown) and cresyl violet staining; coronal section cut at the level of the frontal lobe; layer IV (inner granular layer) is absent in the agranular isocortex of sheep (see Beul and Hilgetag, 2015); WM, white matter. Bottom, confocal image of the first two cortical layers (DCX, white; DAPI, blue). B, DCX+ neurons are present both in paleo- (piriform cortex) and neo-cortex; arrows, type 1 neurons; arrowheads, type 2 neurons (see D). C,D, Main morphological types of the DCX+ neurons (neocortex); type 1: small cell body and simpler apical dendritic arborization (ad); type 2: large cell body and more elaborated apical dendritic arborization (type 2a), also including basal dendrites (bd; type 2b); type 2 cells represent about 7% of total DCX+ cells. Scale bars: 30 μ m.

Figure 4. DCX+ cells in the external capsule of the adult sheep brain. A,C, Numerous clusters of tightly-packed, DCX+ cells are present in most of the external capsule (EC). B, Serial reconstruction showing their distribution and size. Ex, capsula extrema; Am, amygdala; Pu, putamen; Cx, cerebral cortex. C, Examples of DCX+ cell clusters showing different types of organization, spanning from large, tightly-packed cell masses to small groups of dispersed cells. E, The cell clusters occupy empty spaces within white matter areas devoid of astrocytes. Scale bars: 30 μ m.

Figure 5. DCX+ cells in the peri-capsular regions of the adult sheep brain; EC, external capsule; Ex, capsula extrema; Cx, cerebral cortex. A, Groups of scattered, DCX+ cells are present within the amygdala (Am; images in B) and claustrum (Cl, images in C). The morphology of the DCX+ spans from small bipolar to large multipolar in the amygdala (B, bottom; in black, real drawing of some cells; in brown, main cell types); it appears simpler in the claustrum, in which most cells are small unipolar/bipolar and some show simple ramifications (C, bottom right). D, Quantification of the relative amount of different cell types. Scale bars: 30 μ m.

810

811 **Figure 6.** DCX+ cells in the sheep brain at different ages. A, Evident reduction of the amount of
812 DCX+ neurons in the cortical layer II with increasing age is clearly visible after qualitative analysis
813 (top). Quantitative evaluation of DCX+ cell linear density (number of DCX+ neurons in layer
814 II/cortical tract length; bottom) in three cortical regions (red areas) at two brain levels of the
815 newborn and adult sheep: Pc, piriform cortex; Ssg, suprasylvian gyrus; Ccx, cingulate cortex. B,
816 Striking reduction of DCX+ cell populations is clearly evident in the dentate gyrus (DG; note the
817 dilution of the DCX+ cell layer) and subventricular zone (SVZ; note the reduction in thickness of
818 the DCX+ germinal layer) neurogenic sites of neonatal and adult sheep. C, The occurrence,
819 morpholgy, distribution and amount (quantifications on the right; see also Table 3) of DCX+ cells
820 in the sheep capsular/pericapsular regions do not vary significantly at different ages (apart a slight
821 reduction observed in the external capsule, see text). Scale bars: 30 μ m.

822

823 **Figure 7.** DCX+ cells in cortical layer II, external capsule and peri-capsular regions of the adult
824 sheep are non-newly generated. A, Double staining with cell proliferation markers and DCX in the
825 brain parenchyma of the adult sheep: no double stained cells were found in any of the regions
826 investigated (same results with Ki-67 antigen; images not shown). B, BrdU and Ki-67 antigen
827 double staining with DCX in different brain regions of the neonatal brain (after BrdU treatment of
828 the ewes at the second month of pregnancy). Quantification of DCX+/BrdU+ cells in neonatal
829 lambs are represented in pie charts: populations of embryonically-generated cells are detectable
830 both in cortex and in capsular/pericapsular regions. Scale bars: 30 μ m.

831

832 **Figure 8.** Markers of neuronal maturity/immaturity in DCX+ cells of the adult (A,B,D) and young
833 (C,E) sheep brain. A, Double staining for DCX and NeuN (red arrows) in different brain regions;
834 EC, external capsule; Amy, amygdala; Cl, claustrum. B, Both in cortical (Cx) and in
835 capsular/pericapsular regions (Cps), the DCX+/NeuN+ cells represent a small subpopulation of all

DCX+ cells (red areas in pie charts); 1 and 2 in cortex pie chart refer to type 1/type 2 cells (see Fig. 2). C, The marker of initial differentiation and maturity HuC/D is not detectable in the neurogenic sites (DG, dentate gyrus; SVZ, subventricular zone) and mostly absent in DCX+ immature neurons, apart from a weak expression in some type 2 cells of the cortical layer II (circle). D, Double staining with the marker of immaturity PSA-NCAM reveals all DCX+ cells largely decorated in the neurogenic zones (DG and SVZ), whereas only subpopulations of DCX+ cells are partially stained in the cortical and subcortical regions. E, Similarly to PSA-NCAM, the A3 subunit of the cyclic nucleotide-gated ion channel (CNGA3) is detectable in most DCX+ cells of the neurogenic sites and in subpopulations of DCX+ cells in other brain regions. F, Schematic summary of maturity/immaturity features in DCX+ cells of the sheep as revealed by different cellular markers (showed for the cortex but representative of all regions investigated). Scale bars: 30 μ m.

Figure 9. Origin of DCX+ cells by detection of pallial/subpallial markers in the neonatal sheep brain. A, Distribution of *Tbr1* and *Sp8* proteins in different DCX+ cell populations of the cerebral cortex, claustrum, external capsule and amygdala; DCX, white; *Tbr1*, purple; *Sp8*, red. Scale bars: 30 μ m. B, Schematic summary of pallial (purple; SVZ counterpart of dorsal, ventral, lateral, medial pallium) and subpallial (yellow; lateral and medial ganglionic eminences) origin of the DCX+ cells in cortical (Cx) and capsular/pericapsular structures (Cps). Quantification results are reported in pie charts; most of the DCX+ cells in cortex and claustrum are only *Tbr1*+, whereas a mix of *Tbr1*+ and *Sp8*+ cell populations is detectable in the external capsule and amygdaloid nuclei.

Figure 10. Summary and comparative aspects. A, Two main populations of non-newly generated, "immature" DCX+ cells are present in the cerebral cortex and capsular/pericapsular regions of the sheep brain. B, Unlike newly generated neuroblasts of the main neurogenic sites and immature neurons of the cortical layer II, which are consistently reduced with age (see Fig. 5), the amount of DCX+ cells in the sheep capsular/pericapsular regions do not vary from neonatal to adult age. In

862 comparison with results reported for laboratory rodents, our findings in sheep strongly suggests that
863 parenchymal, non-neurogenic structural plasticity (brown areas) can be maintained/increased in
864 large brained, long living mammals, thus following an opposite trend with respect to adult
865 neurogenesis (green). C, Pallial and mixed (pallial and subpallial) origin of the DCX+ cells in
866 different brain regions.

867 Tables

868

869 **Table 1.** Animals used in the present study

870

Source	Sex	Breed	Age	BrdU treatment
INRA Nouzilly (France)	4 M, 3F	Ile-de-France	Neonate (7 days)	Survival: 97 days (injection: 90 days pre-partum)
	3 M		Prepuberal (4 months)	-
	9 F		Adult (2 years)	Survival: 120 days
				Survival: 60 days
				Survival: 30 days

871

872

873

874 **Table 2.** Primary antibodies used in this study

Antigen	Host	Dilution	RRID	Source
BrdU	Rat	1:300	AB_732011	AbDSerotec, Kidlington, UK
DCX	Rabbit	1:3000	AB_732011	Abcam, Cambridge, UK
	Goat	1:2000	AB_2088494	Santa Cruz Biotechnology, Santa Cruz, CA
	Guinea Pig	1:1000	AB_2230227	Abcam, Cambridge, UK
GFAP	Rabbit	1:800	AB_10013382	Agilent Technologies, Carpinteria, CA
	Mouse	1:200	AB_94844	Millipore, Bellerica, MA
Ki-67	Mouse	1:500	AB_393778	Agilent Technologies, Carpinteria, CA
NeuN	Mouse	1:1000	AB_177621	Millipore, Bellerica, MA
Sp8	Rabbit	1:10000	AB_877304	Millipore, Bellerica, MA
Tbr1	Rabbit	1:1000	AB_10806888	Chemicon, Temacula, CA
PSA-NCAM	Mouse	1:1400	AB_95211	Millipore, Bellerica, MA
HuC/D	Mouse	1:800	AB_221448	Invitrogen, Carlsbad, CA
CNGA3	Rabbit	1:250	AB_2039822	Alomone Labs, Israel

875

876

877

878

Table 3. Quantification of DCX+ clusters/cells in the capsular/pericapsular and cortical regions of neonatal and adult sheep brains

A

	Newborn			Adult		
	Area (mm ²)	Number of cells	Density (DCX+ objects/mm ²)	Area (mm ²)	Number of cells	Density (DCX+ objects/mm ²)
External capsule	1,72 ± 0,3	34 ± 4*	19,97 ± 1,4	4,28 ± 0,3	39 ± 7*	9,21 ± 1,6
Clastrum	7,52 ± 0,7	75 ± 22	9,78 ± 2,1	12,56 ± 1,2	77 ± 62	5,86 ± 4,3
Amygdala	11,44 ± 1,0	209 ± 75	18,44 ± 6,9	18,33 ± 3,5	252 ± 18	14,02 ± 2,1
	Length (mm)	Number of cells	Linear density (cells/mm)	Length (mm)	Number of cells	Linear density (cells/mm)
Neocortex	7,20 ± 0,4	329 ± 4	45,69 ± 2,6	9,47 ± 2,4	62 ± 15	6,54 ± 0,5
Paleocortex	4,46 ± 0,3	371 ± 11	83,41 ± 2,3	5,53 ± 0,8	164 ± 68	29,65 ± 7,2

B

	Newborn vs Adults T-tests p values		
	Area (mm2)	Number of cells	Density
Two-way ANOVA	F=5,389; p=0.003	F=136,551; p<0,0001	F=84,258; p<0,0001
External capsule	<0.0001	0.300	0.001
Clastrum	0.003	0.961	0.231
Amygdala	0.030	0.422	0.347
	Number of cells	Length (mm)	Linear density (cells/mm)
Neocortex	<0.0001	<0.0001	<0.0001
Paleocortex	0.164	0.001	<0.0001

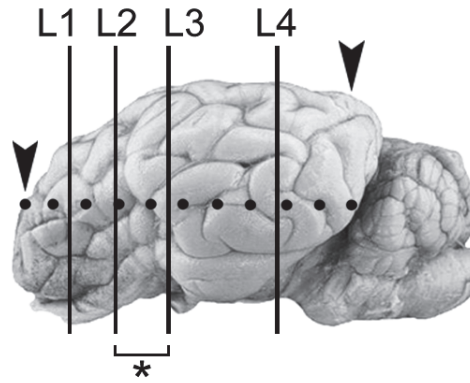
C

Number of cells/objects	Amigdala	Clastrum	EC*	Paleocortex	Neocortex
Amigdala		0.535	0.463	<0.0001	<0.0001
Clastrum	0.535		0.933	<0.0001	<0.0001
EC*	0.463	0.933		<0.0001	<0.0001
Paleocortex	<0.0001	<0.0001	<0.0001		<0.0001
Neocortex	<0.0001	<0.0001	<0.0001	<0.0001	
Density	Amigdala	Clastrum	EC*	Paleocortex	Neocortex
Amigdala		0.923	0.181	<0.0001	<0.0001
Clastrum	0.923		0.055	<0.0001	<0.0001
EC*	0.181	0.055		<0.0001	<0.0001
Paleocortex	<0.0001	<0.0001	<0.0001		<0.0001
Neocortex	<0.0001	<0.0001	<0.0001	<0.0001	

A, Number of DCX+ cells and density in cortical and subcortical regions. *DCX+ objects. B, Two-way ANOVA for all brain regions and T-tests for each region comparing newborn and adult values of perimeter/area, number and density of DCX+ cells. Numbers indicate p values, green and red fill

890 indicate p values lower or greater than 0.05 respectively. C, Pairwise two-way ANOVA analyses of
891 the density and number of DCX+ cells/objects in different brain regions between newborn and adult
892 animals. This analysis compares age related changes between pairs of brain regions, indicated in the
893 first row and column. Numbers indicate p-values for the interaction between age and brain region,
894 significant and non-significant interaction of these two factors are labelled in green and red
895 respectively. Yellow indicate a value that is close to the critical value of 0.05.

A



L1



L2



L3



L4



B

